Advances in Materials
2017; 6(5): 57-65
http://www.sciencepublishinggroup.com/j/am
doi: 10.11648/j.am.20170605.12
ISSN: 2327-2503 (Print); ISSN: 2327-252X (Online)

Dielectrics Properties and Temperature Dependence of Electron Spin Resonance of Doped Molybdenum CCTO

Séka Simplice Kouassi[1, *], Jean-Pierre Sagou Sagou[2], Cécile Autret-Lambert[3], Sonia Didry[3], Marc Lethiecq[3]

[1]Department of Physics Chemistry Mathematics and Computer Science, Jean Lorougnon GUEDE University, Daloa, Ivory Coast

[2]Laboratory of Materials Inorganics Chemistry, Félix Houphouët BOIGNY University, Abidjan, Ivory Coast

[3]Greman Umr 7347 Laboratory, François Rabelais University, Tours, France

Email address:

sekasimplice@yahoo.fr (S. S. Kouassi)

[*]Corresponding author

To cite this article:

Séka Simplice Kouassi, Jean-Pierre Sagou Sagou, Cécile Autret-Lambert, Sonia Didry, Marc Lethiecq. Dielectrics Properties and Temperature Dependence of Electron Spin Resonance of Doped Molybdenum CCTO. *Advances in Materials.* Vol. 6, No. 5, 2017, pp. 57-65. doi: 10.11648/j.am.20170605.12

Received: July 18, 2017; **Accepted**: July 28, 2017; **Published**: August 31, 2017

Abstract: The role perovskite-type $CaCu_3Ti_4O_{12}$ (CCTO) dope by molybdenum (Mo) on the microstructure, dielectric properties and the temperature dependence of Electron Spin Resonance (ESR) has been investigated in this work. The solid state reaction has been used to synthesize CCTO ceramic samples. Substitution on Ti-site by Mo helps to increase the grain size of samples and therefore increase the dielectric constant according to the IBLC theory. There is no great difference between the ESR spectra of pure CCTO and CCTO doped by Molybdenum as a function of temperature. For a given temperature, ESR signal spectrum intensity increases as the Mo content increases. The magnetic susceptibility varies according to the composition only when the temperature is higher than 70K. The antiferromagnetic character of the CCTO decreases when the Mo content increases.

Keywords: Ceramics, Solid State Reaction Method, Dielectric Properties, Magnetic Properties, Electron Spin Resonance

1. Introduction

Research of ultra-miniaturization of electronic devices in the aviation, automotive and mobile phone requires the development of materials with high dielectric constant and stable over a wide temperature range. Dielectric materials commonly used today are ferroelectric oxides such as $SrBi_2Ta_2O_9$, $BaTiO_3$, (Ba, Sr) TiO_3 or relaxor ferroelectrics as Pb $(Mg_{1/3}Nb_{2/3})O_3$. However, these dielectric oxide lack stabilities at high temperature and pressure, or do not have huge dielectric constants. Recently, $ACu_3Ti_4O_{12}$ oxides type with high dielectric constant were found and $CaCu_3Ti_4O_{12}$ (CCTO) [1] presented an exceptional behavior with potential technological applications such as capacitors and microwave devices. Values of dielectric constants of CCTO ranging from 3000 to 300,000 have been reported [2-5] and show that these dielectric properties are very sensitive to manufacturing process, and vary with time, temperature, the sintering atmosphere and the annealing [6]. Authors also report the influence of different doping CCTO solid phase. Thus, while the addition of compounds such as TeO_2, Cerium, Cesium, and Eu_2O_3 greatly reduce permittivity material [7-9], oxides such as P_2O_5, GeO_2, Lu_2O_3 and V_2O_3 increase the dielectric constant [10-13]. When doping is carried out by partial substitution of Ca or Ti sites, we have generally a reduction of the permittivity of the material by substitution on the sites of the first one (Gd et Pr) [14, 15] and an increase on the sites of the second one (Nb, Fe, Co, Ni) [16-17]. In addition, permittivities of these compounds are little more than 40,000 at room temperature and at 1 kHz. Various theories have been developed to explain the high permittivity of the CCTO. It has been proposed that internal insulating barrier (IBLC: Internal Barrier Layer Capacitor) with a structure of conductive grains and insulating grain boundaries is responsible for the high permittivity in polycrystalline ceramics [6, 18]. While other theories suggest the existence

of areas inside the insulating grains CCTO [19] or forming an insulating layer at the interface very fine material / electrodes which induces a polarization phenomenon at the electrodes [20].

The aim of this work is to investigate the influence of a partial substitution of Ti in the structure of CCTO by molybdenum oxide (MoO_3), on the microstructure, the permittivity and temperature dependence of electron spin resonance.

2. Experimental Procedure

The samples in this study were prepared by a conventional solid adapted by using high purity precursors ($CaCO_3$ (99.98%), CuO (99.99%), TiO_2 (99.9%) and MoO_3 (99.99%) previously dried at 400°C for 24h. Stoichiometric amounts of the starting oxides were introduced into polyethylene tube containing zircon beads in the presence of isopropanol. Followed by a grinding in a turbulator for 48 h at a speed of 60 revolutions per minute (rpm), fine powders were obtained after drying of the various mixtures in the oven at 60°C for 3 hours. Compounds $CaCu_3Ti_{4-x}Mo_xO_{12}$ (M_x avec x = 0, 0.05, 0.1) are obtained by calcination at 950°C in air for 12 hours. The chemical reaction occurring during the calcination process can be summarized as follows (equation 1):

$$CaCO_3 + 3CuO + (4\text{-}x)\ TiO_2 + x\ MoO_3 \rightarrow$$

$$CaCu_3Ti_{4-x}Mo_xO_{12} + CO_2 \uparrow \quad (1)$$

Finally, the resulting powders are pressed into pellet diameter of about 10 mm and sintered at 1050°C for 24 hours. The composition of the products was determined by X-ray diffraction using the Bruker AXS D8 diffractometer. Microstructural characterization and elementary analysis of the samples were recorded using scanning electron microscopy (SEM) HITACHI 4160 type having a mounting EDX. Measures of electron spin resonance were performed on different samples with a Bruker EMX 10/2.7 X-band (9.5 GHz). Dielectric measurements were determined in the frequency range of 100 Hz to 1 MHz on perfectly polished pellets faces and on which a layer of gold was raised to establish electrical contact. The PPMS (PPMS, Model 6000) was used to investigate the magnetic properties of samples over a wide temperature band 6K to 350K. The ZFC and FC magnetic measurements were performed. For ZFC, the samples were pre-cooled to room temperature at 6 K without application of magnetic field and then heated by applying a magnetic field of 1000 Oe, the magnetization is measured as a function of temperature. Whereas for FC measurement, the samples are cooled to 6K under action of a magnetic field of 1000 Oe and the magnetization measurement was performed for increasing temperature.

3. Results and Discussion

Figure 1 shows the microstructure of samples M_0, $M_{0.05}$ and $M_{0.1}$ at 1050°C. We observe an increase in average grain size as a function of Mo content, which is mainly due to the decrease in the number of small grains and segregation areas rich in Cu grains boundaries. Table 1 shows the evolution of the grain size according to the Mo contents. Figure 1c with Mo-rich presents grains boundaries well defined and rich in Cu and lack of Mo and Ti as shown by the EDX results (Figure 2). It explains that Mo is preferentially returned in the CCTO structure. At this temperature, CCTO doped with molybdenum has the same effect on the grain growth like GeO_2 and V_2O_3 content obtained in previous studies [11, 13].

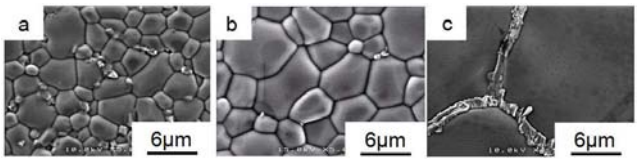

Figure 1. *SEM micrographs at 1050°C of M_0 (a), $M_{0.05}$ (b) and $M_{0.1}$ (c).*

Table 1. *Grain size according to Mo content for 1050°C sintering temperature.*

Grain size (µm)	M_0	$M_{0.05}$	$M_{0.1}$
	3-6	5-10	40-110

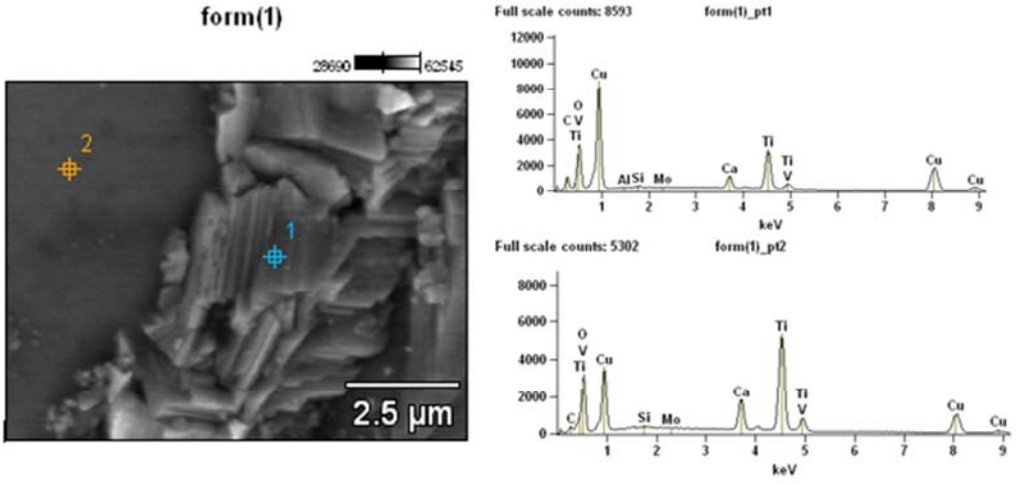

Figure 2. *EDS mapping of $M_{0.1}$.*

X-ray diffraction confirmed the presence of single CCTO phase despite the Mo content (Figure 3). We have no secondary phase or secondary phase is too low to be detected. However, compared with the pure CCTO, we observe a small shift of the peak position for the doped samples. The lattice parameter of pure CCTO (as shown in Figure 3 B) is about 7,394. This value is very close to the results previously reported [21]. The lattice parameter increases slightly with an increase in the concentration of Mo substitution on Ti site. Mo leads to an increase of the lattice parameter due to the difference in their ionic radii which are: 0.605 Å for Ti^{4+} and 0.65 Å for Mo^{4+}.

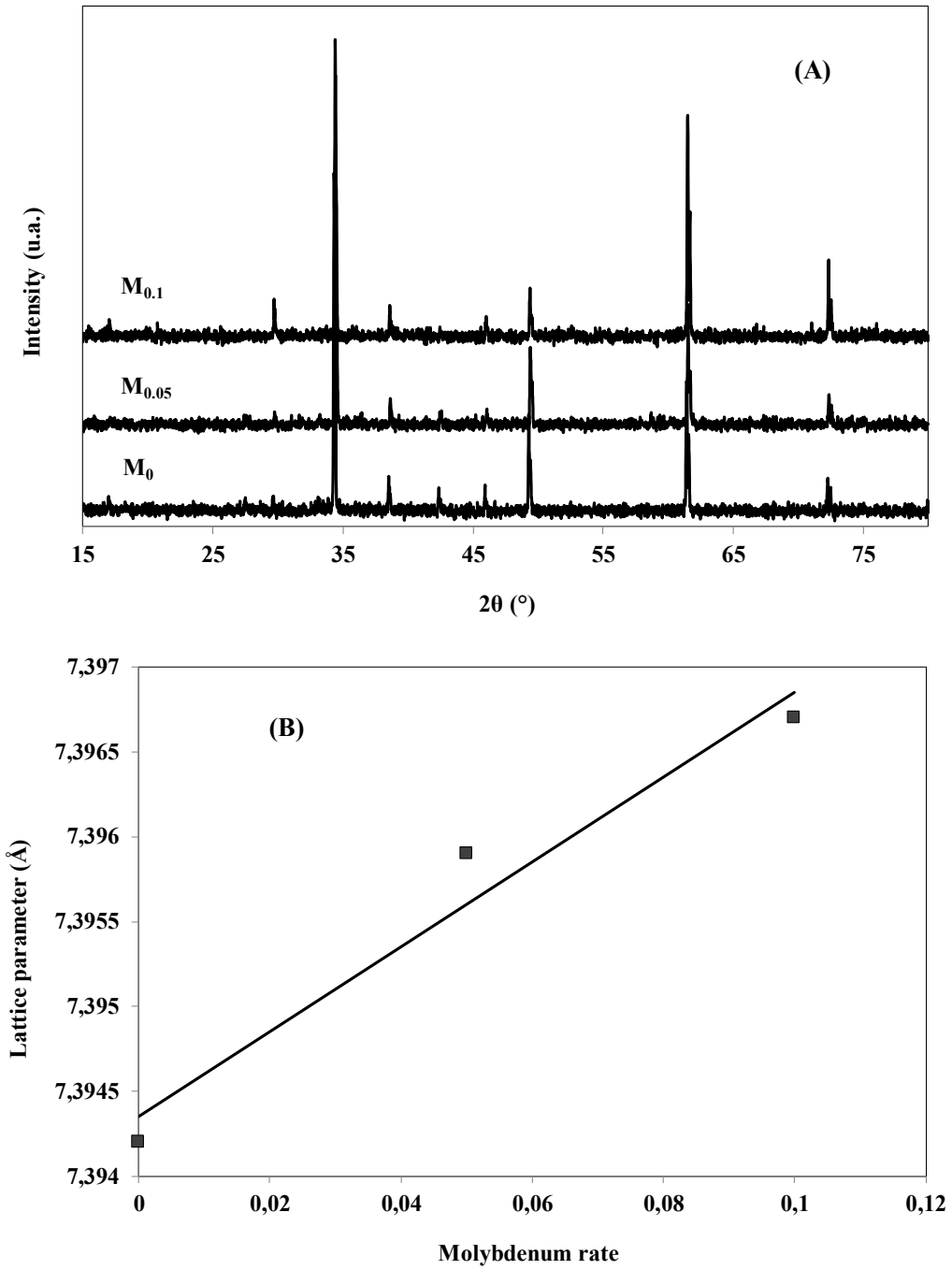

Figure 3. *XRD patterns of M_0, $M_{0.05}$ and $M_{0.1}$ doped samples (A) and lattice parameter depending on molybdenum rate at 1050°C (B).*

Figure 4 shows the change of the dielectric constant and dielectric loss (tan δ) of various compounds M_x measured at room temperature for samples sintering at 1050°C. We observed that for a given frequency, dielectric constant and dielectric loss increase with the molybdenum content (Figure 4A). This result was observed [10-12] for sintering temperatures of various samples doped below 1050°C. The result is in agreement with the theory IBLC which provides an increase in the permittivity when the grain size increases. The increase of the permittivity can be indicated by equation 2:

$$\varepsilon = \varepsilon_{gb}\left(\frac{D}{d}\right) \quad (2)$$

Where D is the grain size, d the grain boundary thickness and ε_{gb} the dielectric constant of grain boundary [7].

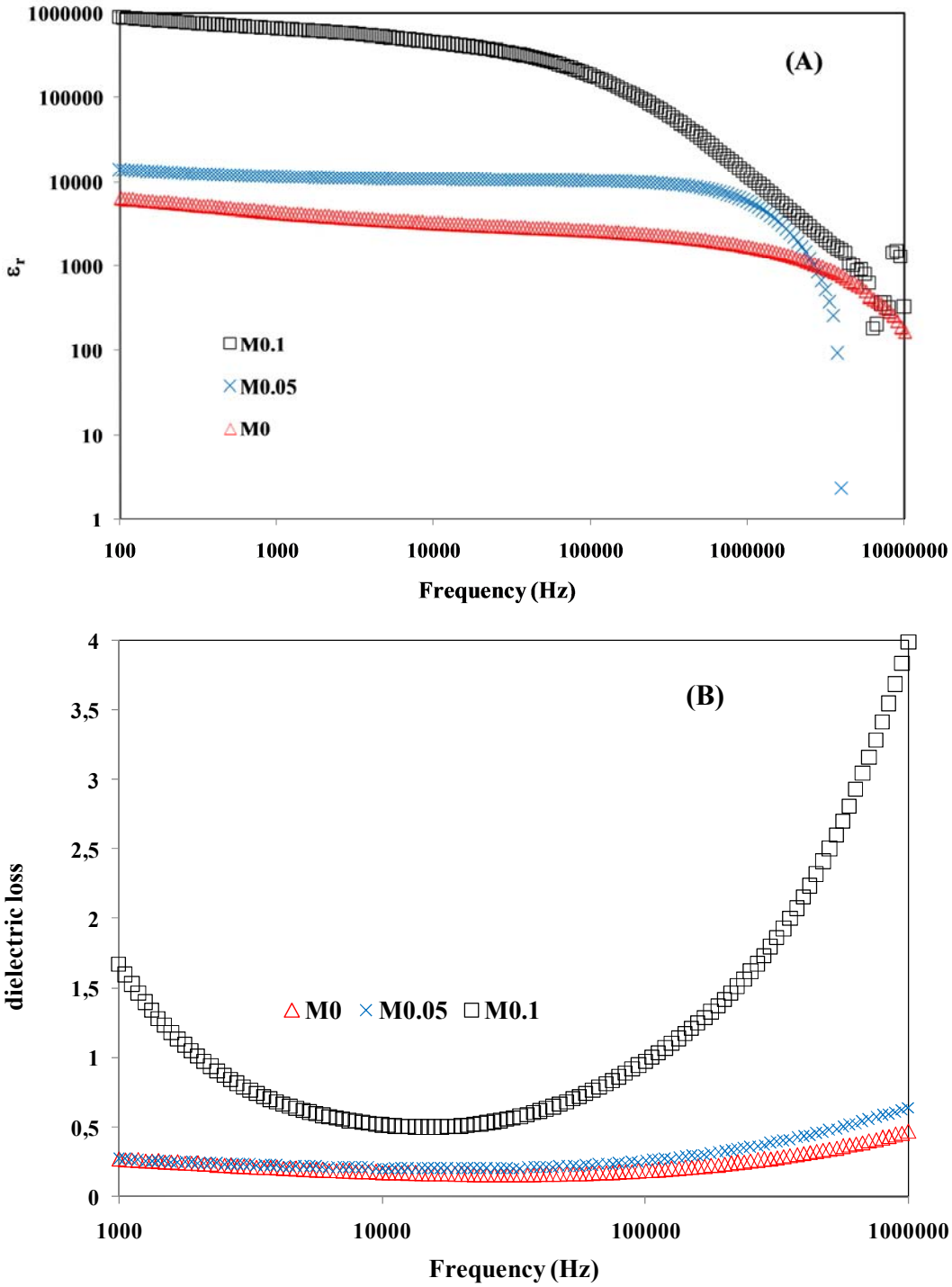

Figure 4. *Frequency dependence at room-temperature of dielectric constant (A) and dielectric loss (B) for the pellets sintered at 1050°C.*

The dielectric loss versus frequency curve (Figure 4B) shows that for a given frequency the dielectric loss increases as the Mo content increases. We can conclude that CCTO doping by partially substitution of Mo on Ti-site has the consequence to increase the dielectric loss.

The ESR spectrum of the pure CCTO consists of a symmetric signal centered at g = 2.15 independent of the orientation of the sample in the magnetic field. Its origin was attributed to the strong delocalization of the hole of the electronic structure of copper $3D^9$ on the four neighboring oxygen ions [22]. ESR spectra can change according to the grain-boundary chemistry [23].

The ESR spectrum of M_x samples sintered at 1050°C was recorded in the temperature range 0 K ≤ T ≤ 300 K (RT: Room temperature) (Figure 5). M_0, $M_{0.05}$ and $M_{0.1}$ have the same ESR signature as a function of time. There is no signal

of grain boundary effect observed in the ESR spectra like shown by Capsoni et al. [23]. Below 25 K where a transition to an antiferromagnetic phase has been reported [24], signal is not apparent. The signal appears only from 25 K, in the paramagnetic field with a Lorentzian line shape. 25 K is the antiferromagnetic (AFM) transition temperature T_N. This value has been reported previously [25].

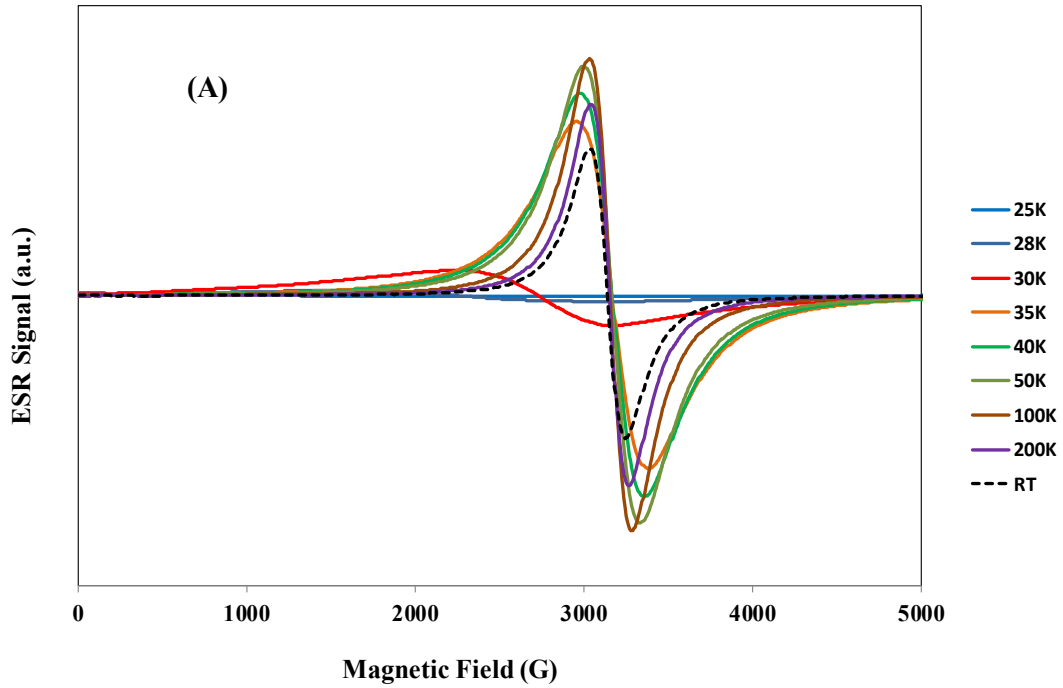

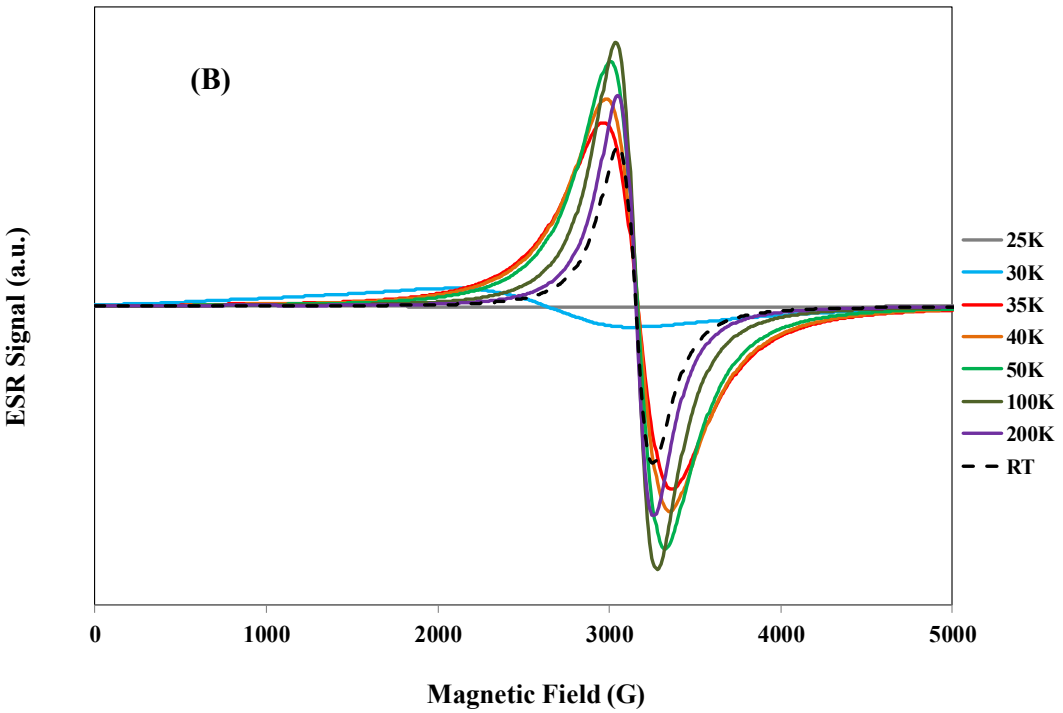

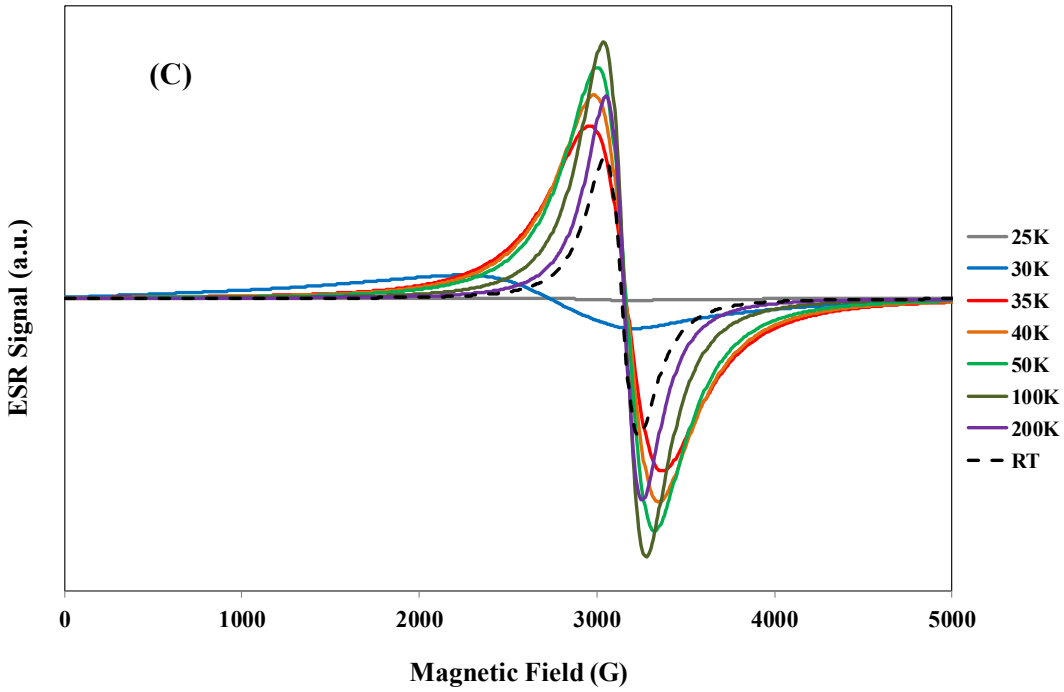

Figure 5. *Temperature dependence of ESR for pellets sintered at 1050°C of M_0 (a), $M_{0.05}$ (b) and $M_{0.1}$ (c).*

Figure 6 shows the evolution of the intensity, the line width (ΔHpp), of effective g factor (g_{eff}) of ESR signal depending on the temperature of the samples M_x. In general, the intensity of the ESR signal increases strongly from 0 to T_N and decreases progressively from T_N to Room Temperature. For a given temperature, this intensity increases as the Mo content increases. The signal intensity is much higher for $M_{0.1}$ versus M_0 and $M_{0.05}$ for a given temperature. ΔHpp and g_{eff} Curves are superimposed for the three samples. We observe a sharp drop ΔHpp and g_{eff} 25K to about 31K (transition range AFM-PM). g_{eff} value remains constant at 2.15 over this temperature while ΔHpp decreases very slightly in this temperature range (paramagnetic).

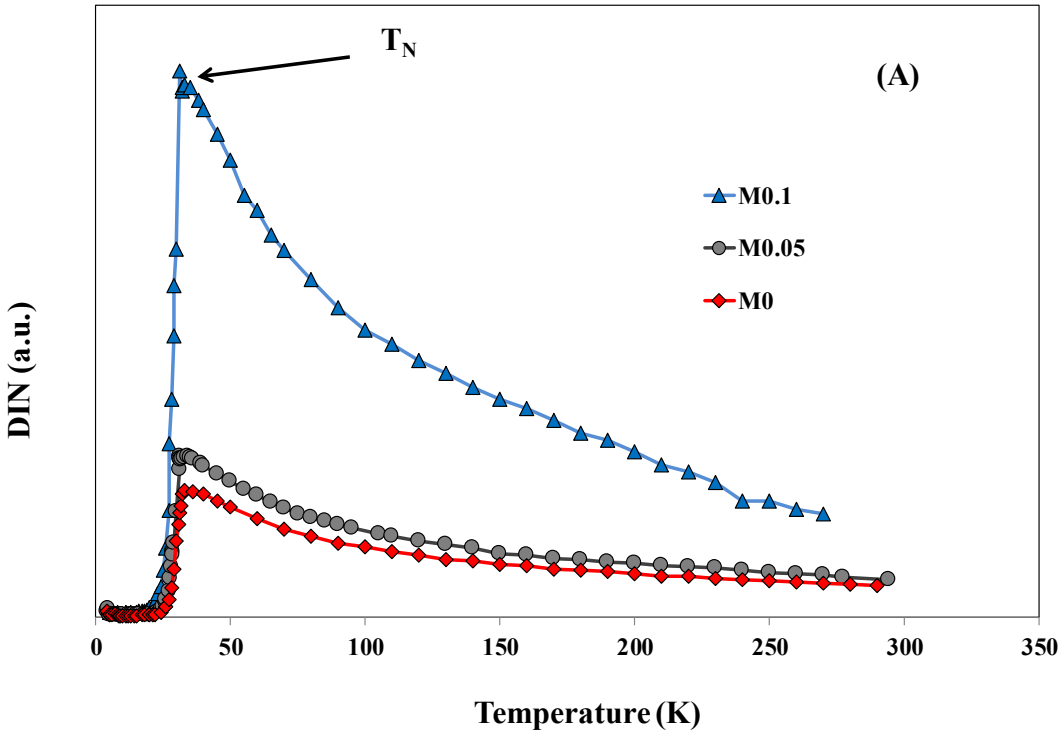

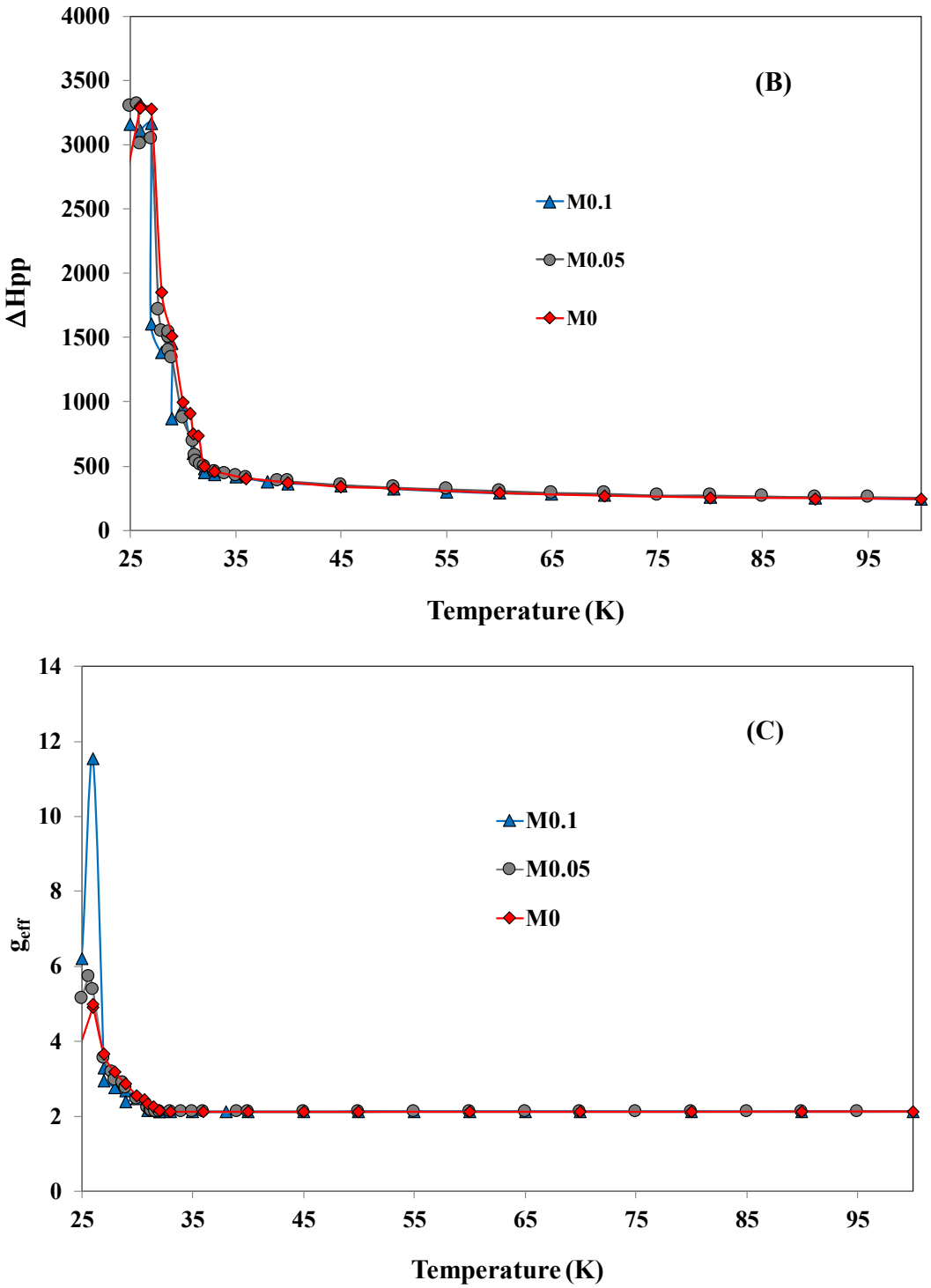

Figure 6. *Temperature dependence of line shape magnitude (a), peak to peak line width (b) and geff-factor (c) of M_x sintered at 1050°C.*

Figure 7 shows the change in function of the temperature of the magnetic susceptibility (ZFC) of samples M_0, $M_{0.05}$ $M_{0.1}$ sintering at 1050°C in a field of 1000 Oe. The magnetic susceptibility is independent on the composition for temperatures below 70K. When the temperature increases (greater than 70K), the magnetic susceptibility decreases as the Mo content increases. The high temperature region (100-350 K) of the reciprocal of the ZFC curve can be fitter according to Curie-Weiss law (equation. 3):

$$\chi = \frac{C}{T-\theta} \quad (3)$$

Where χ, θ and C are respectively the susceptibility, Weiss constant and Curie constant. These constants were determined and their values are listed in Table 2. Two observations are made on θ. θ decreases when Mo content increases for a sintering temperature of 1050°C. We conclude that the antiferromagnetic character of the CCTO decreases when the Mo content increases.

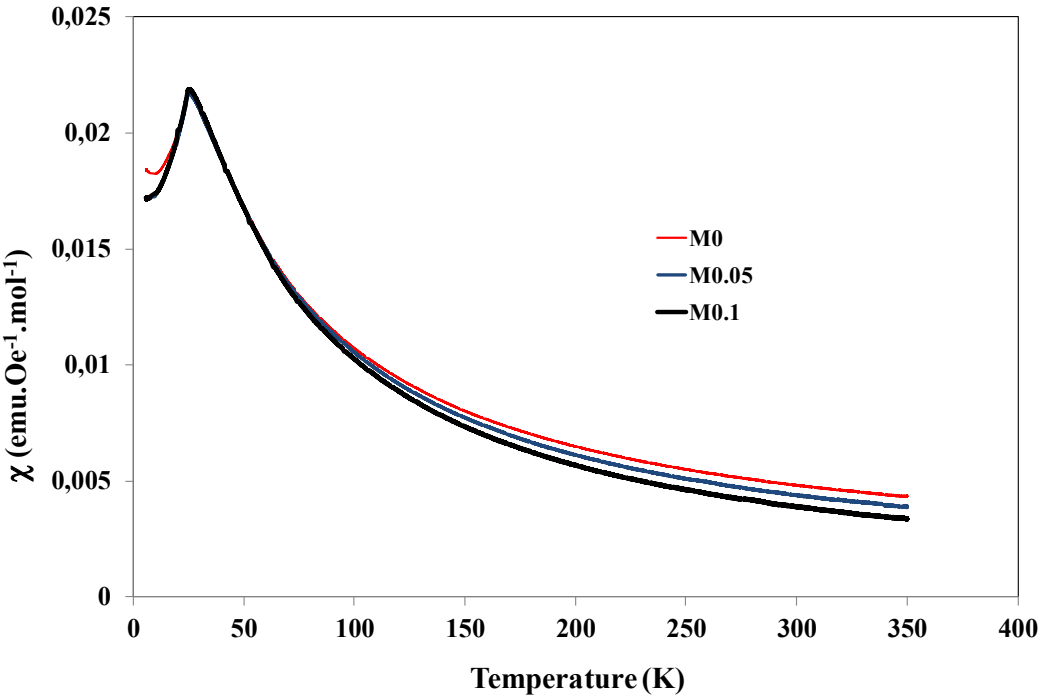

Figure 7. *Temperature dependence of ZFC magnetic susceptibility of M_0, $M_{0.05}$ and $M_{0.1}$ sintered at 1050°C in the field of 1000 Oe.*

Table 2. *Curie and Weiss constants calculated the reciprocal FC curve fitted by Curie-Weiss law.*

	C (curie constant) (emu. K. Oe^{-1}. mol^{-1})	θ (Weiss constant) K
M_0	1.843	-77.53
$M_{0.05}$	1.513	-39.39
$M_{0.1}$	1.349	-26.49

4. Conclusion

Properties of CCTO Mo-doped were studied. The CCTO pure and doped CCTO were prepared by solid route and sintered at 1050°C. At this temperature, substitution on Ti-site by Mo helps to increase the grain size of samples and therefore to increase the dielectric constant according to the IBLC theory. Mo preferentially returned in CCTO structure, and increase slightly his lattice parameter. ESR signal spectrum appear only from 25 K (the antiferromagnetic (AFM) transition temperature TN) and is not influenced by Mo content. For a given temperature, ESR signal spectrum intensity increases as the Mo content increases. The magnetic susceptibility varies according to the composition only when the temperature is higher than 70K. At 70K, it decreases as the Mo content increases. Mo also has the effect to reduce the antiferromagnetic character of the CCTO.

References

[1] M. A. Subramanian, D. Li, N. Duan, B. A. Reisner, A. W. Sleight, High dielectric constant in $ACu_3Ti_4O_{12}$ and $ACu_3Ti_3FeO_{12}$ phases, J. Solid State Chem. 151 (2000) 323-325.

[2] C. Guerrero, J. Roldan, C. Ferrater, M. V. Garcia-Cuenza, F. Sanchez, M. Varala, Growth and characterization of epitaxial ferroelectric $PbZr_xTi_{1-x}O_3$ thin film capacitors with $SrRuO_3$ electrodes for non-volatile memory applications, Solid State Electronics, 45 (2001) 1433.

[3] C. C. Homes, T. Vogt, S. M. Shapiro, S. Wakimoto, A. P. Ramirez, Optical Response of High-Dielectric-Constant Perovskite-Related Oxide, Science 293, (2001) 673-676.

[4] A. F. L. Almeida, R. R. Silva, H. H. B. Rocha, P. B. A. Fechine, F. S. A. Calvalcanti, M. A. Valente, F. N. A. Freire, R. S. T. M. Sohn, A. S. B. Sombra, Experimental and numerical investigation of a ceramic dielectric resonator (DRA): $CaCu_3Ti_4O_{12}$ (CCTO), Physica B 403, (2008), 586-594.

[5] B. A. Bender, M.-J. Pan, The effect of processing on the giant dielectric properties of $CaCu_3Ti_4O_{12}$, Materials Science and engineering B 117, (2005), 339-347.

[6] V. Brizé, G. Gruener, J. Wolfman, K. Fatyeyeva, M. Tabellout, M. Gervais, F. Gervais, Grain size effects on the dielectric constant of $CaCu_3Ti_4O_{12}$ ceramics, Materials science and engineering B, 129, (2006), 135-138.

[7] F. Amaral, L. C. Costa, M. A. Valente, Decrease in dielectric loss of $CaCu_3Ti_4O_{12}$ by the addition of TeO_2, J. Non-Crystalline Solids, 357, (2011), 775-785.

[8] Worawut Makcharoen, Jerapong Tontrakoon, Gobwute Rujijanagul, David P. Cann, Tawee Tunkasiri, Effect of cesium and cerium substitution on the dielectric properties of $CaCu_3Ti_4O_{12}$ ceramics, Ceramics International, 38S, (2012), S65-S68.

[9] Tao Li, Zhenping Chen, Fanggao Chang, Junhong Hao, Jincang Zhang, The effect of Eu_2O_3 doping on $CaCu_3Ti_4O_{12}$ varistor properties, J. Alloys and Compounds, 484, (2009), 718-722.

[10] Sudipta Goswami, A. Sen, Low temperature sintering of CCTO using P_2O_5 as a sintering aid, Ceramics International, 36, (2010), 1629-1631.

[11] F. Amaral, M. A. Valente, L. C. Costa, Dielectric properties of $CaCu_3Ti_4O_{12}$ (CCTO) doped with GeO_2, J. Non-Crystalline Solids 356, (2010), 822-827.

[12] Dong Xu, Biao Wang, Yuanhua Lin, Lei Jiao, Hongming Yuan, Guoping Zhao, Xiaonong Cheng, Influence of Lu_2O_3 on electrical and microstructural properties of $CaCu_3Ti_4O_{12}$ ceramics, Physica B, 407, (2012), 2385-2389.

[13] Séka Simplice Kouassi, Jean-Pierre Sagou Sagou, Cécile Autret-Lambert, Sonia Didry, Anoop Nautiyal, Marc Lethiecq, Effect of Vanadium Doping on Microstructure and Dielectric Behavior of $CaCu_3Ti_4O_{12}$ Ceramics, International Journal of Materials Science and Applications, 6 (1), (2017); 54-64.

[14] Raman Kashyap, O. P. Thakur, R. P. Tandon, Study of structural, dielectric and electrical conduction behaviour of Gd substituted $CaCu_3Ti_4O_{12}$ ceramics, Ceramics International, 38, (2012), 3029-3037.

[15] L. F. Xu, P. B. Qi, X. P. Song, X. J. Luo, C. P. Yang, Dielectric relaxation behaviors of pure and Pr_6O_{11}-doped $CaCu_3Ti_4O_{12}$ ceramics in high temperature range, J. of Alloys and Compounds, 509, (2011), 7697-7701.

[16] Muhammad Azwadi Sulaiman, Sabar D. Hutagalung, Mohd Fadzil Ain, Zainal A. Ahmad, Dielectric properties of Nb-doped $CaCu_3Ti_4O_{12}$ electroceramics measured at high frequencies, J. of alloys and Compounds, 493, (2010), 486-492.

[17] G. Chiodelli, V. Mssaroti, D. Capsoni, M. Bini, C. B. Azzoni, M. C. Mozzati, P. Lupotto, Electric and dielectric properties of pure and doped $CaCu_3Ti_4O_{12}$ perovskite materials, Solid state Communications, 132, (2004), 241-246.

[18] A. R. West, T. B. Adams, F. D. Morrison, D. C Sinclair, Novel high capacitance materials: - $BaTiO_3$: La and $CaCu_3Ti_4O_{12}$, J. Eur. Ceram. Soc. 24, (2004), 1439.

[19] T.-T. Fang et H.-K. Shiau. Mechanism for developing the boundary barrier layers of $CaCu_3Ti_4O_{12}$, J. Am. Ceram. Soc. 87, (2004), 2072-2079.

[20] P. Lunkenheimer, R. Fichtl, S. G. Ebbinghaus, A. Loidl. Non-intrinsic origin of the Colossal Dielectric Constants in $CaCu_3Ti_4O_{12}$, Phys. Rev. B, 70, (2004).

[21] A. Sen, U. N. Maiti, R. Thapa, K. K. Chattopadhyay, Effect of vanadium doping on the dielectric and nonlinear current–voltage characteristics of CaCu3Ti4O12 ceramic, J. alloys and Compounds, 506, (2010), 853-857.

[22] M. C. Mozzati, C. B. Azzoni, D. Capsoni, M. Bini, V. Massaroti, Electron paramagnetic resonance investigation of polycrystalline $CaCu_3Ti_4O_{12}$, J. Phys. Condens. Matter 15, (2003), 7365-7374.

[23] D. capsoni, M. Bini, V. Massarotti, G. Chiodelli, M. C Mozzatic, C. B. Azzoni, Role of doping and CuO segregation in improving the giant permittivity of $CaCu_3Ti_4O_{12}$ J. Solid State Chem., 177 (2004), 4494.

[24] A. Koitzsch, G. Blumberg, A. Gozar, B. Dennis, A. P. Ramirez, S. Trebst, S. Wakimoto, Antiferromagnetism in $CaCu3Ti_4O_{12}$ studied by magnetic Raman spectroscopy, Phys. Rev. B, 65, (2002), 524061.

[25] Virginie Brizé, Cécile Autret-Lambert, Jérome Wolfman, Monique Gervais, Patrick Simon, François Gervais, Temperature dependence of electron spin resonance in $CaCu_3Ti_4O_{12}$ substituted with transition metal elements, Solids State Sciences, 11, (2009), 875-880.